CASPER: A modelling framework to link mineral carbonation with turnover of organic matter in soil

Computers and Geosciences 124 (2019) 58–71

Contents lists available at ScienceDirect

Computers and Geosciences

journal homepage: www.elsevier.com/locate/cageo

Research paper

CASPER: A modelling framework to link mineral carbonation with the turnover of organic matter in soil

B.W. Kolosz[a,b,*,1], S.P. Sohi[c,2], D.A.C. Manning[a,3]

[a] School of Natural and Environmental Sciences, Newcastle University, United Kingdom
[b] Research Centre for Carbon Solutions, Heriot-Watt University, United Kingdom
[c] School of GeoSciences, University of Edinburgh, United Kingdom

ARTICLE INFO

Keywords:
Soil inorganic carbon
Carbon capture
Soil carbon modelling
Mineral weathering

ABSTRACT

Rapid formation of stable soil carbonates offers a potential biologically-mediated strategy for removing atmospheric CO_2 and forms a part of the negative emissions debate in a bid to maintain global temperatures of 1.5 °C. Microbial respiration in soil and respiration by plant roots leads to high partial pressure of CO_2 below ground. Given adequate supply of calcium in soil solution the sequestration of C into the mineral calcite ($CaCO_3$) can occur at rapid rates. We have coupled an established soil C model *RothC* to a simplified geochemical model so that this strategy can be explored and assessed by simulation. The combined model *CASPER* partitions CO_2 respired belowground into soil solution as HCO_3^- and simulates its reaction with Ca^{2+} based on a particular dissolution rate for Ca-bearing minerals, with precipitation of calcite into soil pores as a consequence. Typical model output matches observed field rates of calcite accumulation over 5 years, namely 81 t ha^{-1}, with 19 t CO_2 ha^{-1} sequestered into the soil.

1. Introduction

The Intergovernmental Panel on Climate Change (IPCC) has highlighted the need for CO_2 removal in avoiding a rise in global temperature more than 1.5 °C relative to pre-industrial times (IPCC, 2018). As well as accumulating organic C in soil, atmospheric carbon dioxide (CO_2) can be removed by enhanced rock weathering (Beerling et al., 2018), or by precipitation of inorganic C as soil carbonate minerals (Manning and Renforth, 2012). Carbonate minerals in soil naturally store as much C as is present in the atmosphere, and possibly as much as exists in soil organic carbon (SOC) pools (Lal and Kimble, 2000). Since the source of C in this pool is largely from CO_2 produced in the organic soil C cycle (i.e. pedogenic, formed in soil), there is both the potential to facilitate rapid increases in stable inorganic C observed in managed land (Washbourne et al., 2015), and to develop predictive capacity through model development.

The equilibrium content for organic C in soil is defined by the balance between inputs of C from plant roots and above-ground residues, and the decomposition of this plant material by soil micro-organisms. A number of models are available to predict changes in SOC in space and time, with relevance to planning land use and soil management. These models account in a simplified way for the turnover and stabilisation that occurs during decomposition, in response to plant productivity, climate and soil texture. Examples of such models include Roth C, CENTURY (Paustian et al., 1992; Parton, 1996) and DAISY (Mueller et al., 1996). For inorganic C in soil there are no corresponding models available to guide decision making and policy. In this paper, we describe *CASPER* (**C**arbonate **A**ccumulation in **S**oils through the **P**rediction of **E**lemental **R**elease). It is a first attempt to simulate the irreversible one-way accumulation of inorganic C from CO_2 in the presence of calcium bearing precursors and is thus quite distinct from SOC. Development of the CASPER model should permit integrated approaches to land management for C storage, where the supply of calcium from mineral sources is managed in order to promote precipitation of the carbonate mineral calcite ($CaCO_3$).

Our approach is to draw on existing simulation of the CO_2 produced in organic C decomposition (and from plant root respiration), to create a simple new model of calcite saturation. As with the organic C model, the inorganic model requires only a limited amount of site-specific data in order to run (APHA, 2012). The stock of calcium-bearing minerals is

* Corresponding author. School of Natural and Environmental Sciences, Newcastle University, United Kingdom.
E-mail address: b.kolosz@hw.ac.uk (B.W. Kolosz).
[1] Ben Kolosz contributed to establish the basis of CASPER and was responsible for all modelling.
[2] Saran Sohi contributed to the linkage of soil organic carbon turnover and the CO_2 production model.
[3] David Manning contributed to the design of the geochemical model and was project lead.

https://doi.org/10.1016/j.cageo.2018.12.012
Received 9 September 2018; Received in revised form 19 December 2018; Accepted 23 December 2018
Available online 05 January 2019

one input variable. Slow dissolution of these minerals releases Ca^{2+} while generation of HCO_3^- is driven by CO_2 simulated by the organic carbon model (and plant root respiration). When soil solution reaches saturation with respect to calcite it precipitates. Calcite forms at maximum rate when the soil CO_2 is maintained at the partial pressure necessary to maintain precipitation at the rate constrained by calcium release by mineral dissolution. There is clear dependence on Ca^{2+} availability and the dissolution rate of the Ca-bearing minerals.

Natural landscapes that display a high concentration of inorganic C formed in soil pedogenic inorganic carbon, (PIC) are associated with arid and semi-arid climates, where restricted soil water favours the accumulation of Ca^{2+} in soil profiles. These landscapes account for most PIC globally, though pedogenic carbonates occur quite widely in low concentrations. Statistical models have been used to estimate national SIC stocks based soil on Ca and Al concentrations (Rawlins et al., 2011; Marchant et al., 2015), but there is a lack of models that simulate carbonate C formation through an integrated understanding of physical, chemical and biological processes. The need for such models arises in large part from the observation that formation of PIC can be extremely rapid in managed land. This has highlighted the opportunity to sequester large amounts of CO_2 into calcite even in a small area and over short timeframes (Washbourne et al., 2012, 2015; Jorat et al., 2015a,b; Renforth et al., 2011b). In particular, Washbourne et al. (2012) measured an increase in PIC 23 t C $ha^{-1}yr^{-1}$ at an urban site containing calcium-containing demolition fines. This is a considerably greater amount than can be achieved, for example, by the capture of CO_2 into standing plant biomass in woodland establishment. The sources of calcium in demolition fines arise from concrete structures and include calcium silicates and hydroxides within Portland cement, and gypsum (calcium sulfate) derived from plaster. The pedogenic origins of calcite in the study of Washbourne et al. (2015) could be confirmed by stable isotope analysis, using the distinction in $^{12:13}C$ (stable isotope) ratio between plant-fixed organic C and C in CO_2 directly from air. This evidence was corroborated by ^{14}C dating, which showed notable proportions of modern C. Other work has shown that carbonate minerals can form in artificial soils where green waste compost is mixed with finely ground natural calcium silicates such as dolerite quarry fines (Manning et al., 2013). In this case, C accumulated as PIC (4.8 tC $ha^{-1}yr^{-1}$), again confirmed using stable isotope data (Manning et al., 2013).

In idealised form, the reaction (1) between calcium silicate minerals and CO_2 can be written as follows:

$$CaSiO_3 + CO_2 + 2H_2O \rightarrow CaCO_3 + H_4SiO_4 \text{ (Reaction 1)}$$

As well as predicting PIC accumulation based on dissolution rates that apply in the field, more accurate estimates of dissolution may be established through model parameterisation. This is a key objective in the initial development of *CASPER*. Once parameterised, such models could enable further development and eventual use of engineered soils to address the challenging and increasingly important need for greenhouse gas removal (GGR) through PIC formation.

CASPER therefore addresses a particular gap in current modelling and prediction for GGR opportunities, with the potential to integrate further options such as biochar C storage. It is currently designed to simulate situations where crushed rock is used as a component of artificial soil or as an amendment to natural soils. Through calibration against data on measured capture into artificial soils of known history, *CASPER* aims to permit the establishment of distinct *in-situ* dissolution rates for a limited range of mineral mixtures and site-specific circumstances. These mixtures may include construction and demolition waste, fly ash and iron and steel slags, which have all been found to enhance C capture and storage in urban settings (Renforth et al., 2009, 2011a,b; Morales-Flórez et al., 2011; Mayes et al., 2018). Accumulating PIC using basaltic and doleritic quarry fines as a Ca source (fine particles produced during the manufacture of widely used construction aggregates) extends the approach to settings where application of demolition materials might not be permitted (Manning et al., 2013). In this paper we introduce *CASPER* and report on the inference of dissolution rates as well as the characteristics of model output.

2. Model description

CASPER is based on a novel extension of an existing soil CO_2 production model (Roth C) with a simplified geochemical dissolution and precipitation model. The latter was originally developed by the American Public Health Association (APHA, 2012) and is ideal for circumstances where compositional data for the soil solution of interest is limited. The sources of elevated CO_2 (up to a hundred-fold) in soil are microbial respiration of plant-derived organic matter (substrate) affected via compost layers and the respiration of active root systems. Geochemical release of Ca depends on the dissolution of non-carbonate Ca-bearing minerals. Calcite precipitates in soil pores when the concentrations of Ca^{2+} and HCO_3^- ions in solution reach a threshold concentration, i.e. is saturated with respect to calcite. The model is currently implemented using the graphical system dynamics software Vensim v7.1 (Eberlein and Peterson, 1992) and a range of input parameters pre-calculated using Excel. Table 1 illustrates model nomenclature used within the paper and appropriate section numbers and Fig. 1 illustrates an overview of the complete model.

2.1. CO_2 production model

RothC 26.3 is used to predict the CO_2 flux arising from organic C turnover in soil (Coleman and Jenkinson, 1996). RothC has a simple structure and a limited set of driving variables but its output compares well with more complex models (Smith et al., 1997). Other models have arisen from using Roth C as their foundation for similar work. Bonten et al. (2016) predicted the effects of acid deposition from the atmosphere on C sequestration, eutrophication and soil pH. Mondini et al. (2017) proposed modifying the Roth C model in order to improve the definitions of exogenous organic matter quality (i.e. degradability of compost and manure inputs), so that the mineralisation of soil C could be more accurately predicted. Skjemstad et al. (2004) considered the effect of naturally high concentrations of charcoal in Australian soils to propose a revision to initialisation.

2.1.1. CO_2 flux from plant litter and exudates

Plants deposit organic C into soil through litterfall aboveground and the belowground input of root litter. Belowground plant roots also exude C directly into the soil. These materials are substrates for soil micro-organisms, which through a process of repeated substrate utilisation and stabilisation slowly return the C to the atmosphere in their respiration and turnover. *RothC* simulates this process primarily to predict the equilibrium soil content of organic carbon, (area-based stocks of SOC, tC ha^{-1}), but CO_2 is a resulting output. Roth C assumes using its standard land management and weather files that the five SOC pools will not reach equilibrium until approximately 10,000 years after soil has been freshly placed. To account for the contrasting composition of organic C entering soil and the progressive stabilisation of residual C, RothC invokes three compartments of contrasting turnover rate, supplied by two source (input) pools. The input pools represent plant-derived C in litter and exudates, differentiated by their quality as microbial substrate. The partitioning between decomposable plant material (DPM) and resistant plant material (RPM) has been obtained through calibration and reflects differences in the chemical composition of

Table 1
Model nomenclature.

Symbol	Description	Equation number
CO_2 dissolution (2.1.4):		
K_{CO2}	Henry's law constant	Eq. (1) and (2)
P_{CO2}	Partial pressure of CO_2 in Atm	Eq. (1) and (2)
pK_{CO2}	CO_2 linear constant function	Eq. 3
Release of Ca from Silicate minerals (2.2.1):		
G_d	Average grain diameter	Eqs. (4), (5) and (9)
G_v	Spherical grain volume	Eqs. ((4), (6), (8) and (10)
G_m	Mass of one grain	Eq. 6
G_{kg}	Amount of grains per Kg	Eq. 6
SA_g	Grain surface area	Eq. 5
SUB_d	Substrate depth	Eq. (7) and (8)
SUB_v	Substrate volume	Eq. 7
G_{ha}	Grains per ha	Eq. (8) and (10)
STO_{tha}	Total stock of an element in tonnes	Eq. 11
D	Substrate density	Eq. 11
COM_{wt}	Chemical composition	Eq. 11
Weathering of silicate minerals and mass transfer (2.2.2):		
R	Chemical weathering rate (mol m^{-2} s^{-1})	Eq. 12
ΔM	Change in Solute mass (mol) from weathering	Eq. 12
S	Total surface area	Eq. 12
t	Reaction duration	
Ionic strength and equilibrium concentrations (2.2.3):		
CBE	Charge balance error	Eq. 15
T	Temperature	Eqs. (16) and (17)
pK_2	Negative log [-log] of the secondary dissociation constant	Eqs. (16) and (23)
pK_c	Negative log of calcite ionisation constant	Eqs. (17) and (23)
fi	Activity coefficient	Eqs. (18) and (23)
$[X]$	Molar concentration of X	Eq. 18
(X)	Activity of ion X	Eq. 18
I	Ion of a particular element	Eq. 20
c_i	ion I molar concentration	Eq. 20
z_i	Ion charge number	Eq. 20
μ	Ionic strength	Eq. 21
A	Constant estimated from dielectric constant and temperature	Eq. 19
Calcite precipitation (2.2.4):		
IAP	Ion activity product	Eq. 22
K_{sp}	Solubility product	Eq. 22
SI	Calcite saturation index	Eqs. (22) and (24)
pH_s	Saturated pH value	Eqs. (23) and (24)
pH	Actual pH	Eq. 24
$[pCa_2+]$	Negative log of free calcium ions	Eq. (23)
$[pHCO_3-]$	Negative log of bicarbonate ions	Eq. (23)

different plant inputs. The remaining soil pools comprise humified organic matter (HUM), inert organic matter (IOM) and the microbial biomass itself (BIO). Microbial biomass (BIO) acts on all pools (except IOM) as microbial substrates and follows first-order reaction kinetics. Carbon dioxide is the product alongside new BIO (assimilated carbon) and new HUM (residual C substrate). BIO is itself a substrate since the microbial population has its own rate of turnover (producing further BIO alongside CO_2 and HUM). The small IOM pool is considered inert, i.e. is not utilised by micro-organisms at a rate relevant to simulation timescales. It has been likened to fire-derived black C or charcoal. The biological decomposition process simulated by RothC is influenced by soil moisture and temperature conditions, for which modifiers are applied. The presence of plant cover invokes a further modifier to decomposition rate, i.e. a modifier to the rate of soil drying (evapotranspiration) in order to reflect the transpiration component.

2.1.2. CO_2 flux from root respiration

In an equilibrium situation with respect to plant and soil (i.e. when plant biomass is mature and where there is no removal through harvest), there should be no inter-annual variation in plant biomass, the annual C input to soil, or the soil C content. Based on the magnitude of global net primary production (annual biomass growth, NPP) and global respiration (gross primary production, photosynthesis, GPP), and assuming roots account for about half of total plant respiration (based on relative biomass), root respiration should be approximately half as large as the input of organic C to soil (and thus also half the output of CO_2 respired by micro-organisms). In a situation where biomass is re-establishing or where biomass is harvested, root respiration will be a larger proportion (NPP is a larger proportion of GPP, with either net biomass accumulation or constant biomass removals). To reflect this principle and for simplicity, we simply assume for our initial simulations that the respiration of roots is equal to NPP (total plant C input).

2.1.3. Soil CO_2 partial pressure

CO_2 dissolution is affected by partial pressure, according to Henry's Law. We assume that the soil is at field capacity i.e. 60% water holding capacity. CO_2 partial pressure is assumed to be 1 atm, as RothC predicts more evolved CO_2 than can be accommodated by the available pore space (assuming 25% porosity) at atmospheric pressure (1 m soil depth). The excess is a flux that leaves the soil. At field capacity, partial pressure remains constant at 1, however, at soil saturation (> 90% moisture content, < 10% pore head space) partial pressure fluctuates between 1 and 2 atm. It is assumed however that in most cases there is enough CO_2 available in order to drive the model, as calcium is rate limiting.

2.1.4. CO_2 dissolution

HCO_3- concentration in the soil solution is calculated assuming total soil porosity of approximately 25% for a soil made by blending solid particles (Jorat et al., 2015b). CO_2 dissolution is calculated using Henry's law (Sander, 2014). Equilibrium in terms of atmospheric and dissolved CO_2 with partial pressure (P_{CO2}) is defined through the following equation:

$$[CO_2] = K_{CO2} \cdot P_{CO2} \quad (1)$$

K_{CO2} is the Henry's Law constant and P_{CO2} is partial pressure. Since there is a constant ratio $[H_2CO_3]/[CO_2]$ with an independence in terms of temperature between 0°C and 50 °C (Lowenthal and Marais, 1976):

$$[H_2CO_3^*] = K_{CO2} \cdot P_{CO2} \quad (2)$$

The constant K_{CO2} is temperature dependent and given by the linear function (Lowenthal and Marais, 1976):

$$pK_{CO2} = 1.12 + 0.0138^*T \text{ within the range } 0°C - 35°C \quad (3)$$

In order to determine the equilibrium of CO_2 between the water and the atmosphere, there is a direct relationship between alkalinity and pH (Weber and Stumm, 1963). We assume that the dissolution of CO_2 takes place in an open system, which means that the soil solution in contact with exogenous CO_2 from SOM is slightly acidic (pH 5.61), and that the dominant dissolved carbonate species is HCO_3^-.

2.2. Geochemical model

2.2.1. Release of Ca from silicate minerals

Calcium silicate minerals either introduced to the soil substrate or mixed with organic matter to produce an artificial soil weather at specific rates and release Ca^{2+} and other elements to the soil solution. Previous observation suggests extremely slow rates of Ca^{2+} release (e.g. Palandri and Kharaka (2004)). Such rates are far too slow to explain the PIC accumulation reported above for urban soils or artificial mixes of compost and crushed dolerite. The rates of dissolution, i.e. the

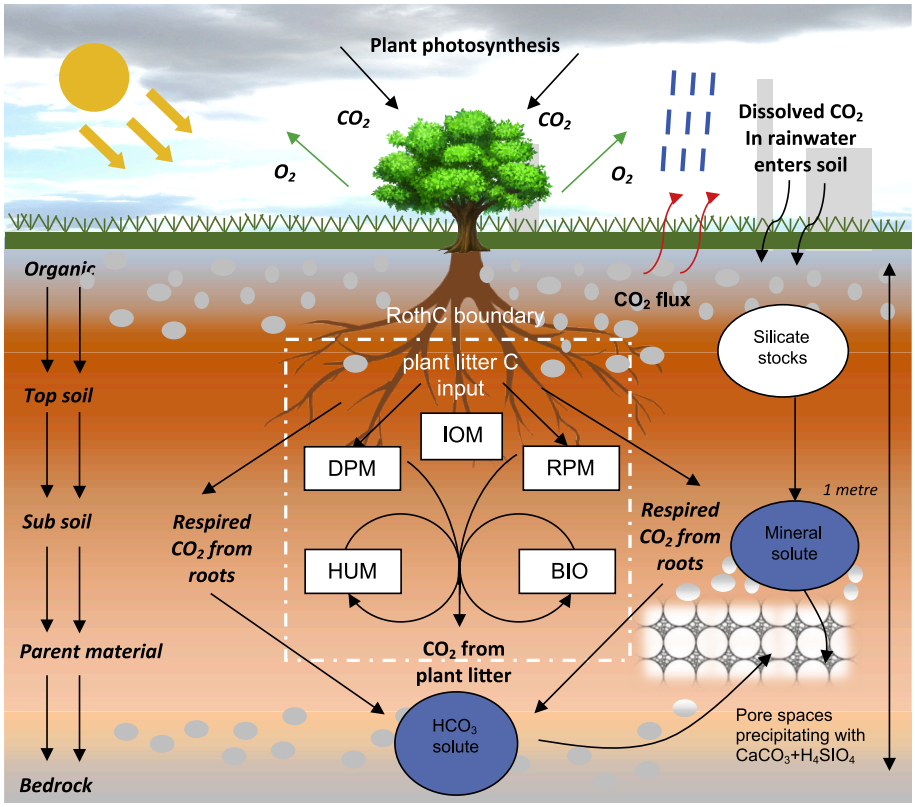

Fig. 1. Structure of RothC organic carbon pools and geochemical model in CASPER (IOM: Inert organic matter; DPM: Decomposable plant material; RPM: Resistant plant material; BIO: Microbial biomass; HUM: Humified organic matter).

weathering rates, depend on the surface area of the soil minerals that is available for reaction. Overall, to address calcium dissolution at a field scale and to integrate with RothC, it is expressed per ha of land area. *CASPER* considers the release of Ca^{2+} from individual grains of a specific size, summed to evaluate total release per hectare. The total mineral grain surface area per ha is estimated geometrically assuming spherical grains. To calculate the elemental stocks in moles per ha, we must first calculate grain volume and surface area:

$$\frac{4}{3}\pi\left(\frac{G_d}{2}\right)^3 = G_v \tag{4}$$

$$4\pi\left(\frac{G_d}{2}\right)^2 = SA_g \tag{5}$$

Where G_d is the average grain diameter of the substrate that is divided by 2 to obtain the grain radius and G_v is the spherical grain volume (mm^3). The surface area (mm^2) of the grain SA_g is also derived from the radius. To obtain the quantity of grains per kg of granular rock material:

$$G_v \cdot G_m \cdot 1\,000 = G_{kg} \tag{6}$$

Where G_m is the mass of 1 grain and G_{kg} is the number of grains per kg. Substrate volume per ha is calculated in m^3 through:

$$100^2 \cdot SUB_d = SUB_v \tag{7}$$

1ha = 10 000 m^2 (100 × 100) multiplied by SUB_d which is the user defined substrate depth (for example 1 m) and SUB_v is the final volume of the substrate. Total grains per ha G_{ha} is calculated through equation (16).

$$G_{ha} = \left(\frac{1\,000^3}{G_v}\right) \cdot SUB_d \tag{8}$$

Total elemental stocks are in tonnes per ha (STO_{tha}). For simplicity at this stage, it is assumed that each spherical grain reacts through a near-surface shell (dissolution rates are slow, so reaction of the entire grain is limited):

$$SP_i = \frac{4}{3} \cdot \pi \cdot \left(\frac{G_d}{2} - 0.01\right)^3 \tag{9}$$

$$VD_{ha} = G_{ha} \cdot \left(\frac{G_v - SP_i}{1\,000^3}\right) \tag{10}$$

$$STO_{tha} = (VD_{ha} \cdot D \cdot 1\,000) \cdot \frac{COM_{wt}}{100\,000} \tag{11}$$

Where SP_i is the inner sphere of the grain shell G_v represents the radius of the grain and also the radius of the outer sphere. SD is the shell depth and VD_{ha} is the volume of the dissolved shell per ha (m^3), D is the density of the substrate (approximately 2.7 g/cm^3 for basalt). COM_{wt} is the chemical concentration for the selected element.

2.2.2. Weathering of silicate minerals and mass transfer

CASPER simulates the process of chemical weathering in terms of silicate minerals, and ignores physical weathering, which in soils is hard to predict. The chemical weathering rate R (mol m^{-2} s^{-1}) of silicate minerals is illustrated by the following relationship:

$$R = \frac{\Delta M}{St} \tag{12}$$

ΔM (mol) is the change in concentration in solution over time, S (m^2) is total surface area of the dissolving grains, and t (s) is the duration of the reaction.

2.2.3. Ionic strength and equilibrium concentrations

The simplified geochemical model (APHA, 2012) used in this study requires an estimate of ionic strength and chemical composition of the

Table 2
Data requirements and causal influences.

Criteria	Value	Initial data requirements	Modelled causal influences
Clay content of the soil	%	Soil type, $CaCO_3$ content	Evolved CO_2/HCO_3 production
DPM/RPM Ratio	< 0–1 >	Soil type	Evolved CO_2/HCO_3 production
Average monthly mean air temperature	ºC	Local temperature	Calcite saturation index, Soil organic decomposition rates
Soil Cover	Cover Material	Vegetation in substrate	Soil Organic decomposition rates, Evolved CO_2/HCO_3 production
Monthly input of plant residue	t C ha^{-1}	Vegetation in substrate	Evolved CO_2/HCO_3 production
Depth of soil layer sampled	m	n/a	Silicate mineral stocks
Silicate mineral stocks	t/ha	Substrate density, grain diameter, shell depth	Weathering rate
Soil porosity	%	Density of Basalt (2.7 g/cm^3)	Moisture content, pore head space
Shell depth	mm	Mineral composition	Mineral stocks, release rate
Substrate density	g/cm^3	Mineral composition	Mineral stocks, Soil porosity
Grain diameter	µm-mm	Clay fraction particle size of soil	Mineral stocks, release rate
Elemental weathering rate	mol m^{-2} s^{-1}	Sampled rates (Hausrath et al., 2009), Soil moisture deficit, Pore space	Calcite dissolution, Mineral stocks
Soil solution composition	mM	Sampled (Benians et al., 1977)	Ionic strength
Soil pH	1–10	Sampled (Benians et al., 1977)	Calcite saturation index
Atmospheric pressure	Atm	Soil moisture content, Substrate density	CO_2 dissolution/HCO_3 production

soil solution so that the saturation index (SI) of calcite can be determined. The most abundant cations that affect ionic strength are Ca, Mg, Na and K, therefore only these specific elements were considered in the model. Initial concentrations of HCO_3^- were also used, while charge balance is assumed to be as chloride, Cl^-, calculated using molar concentrations:

$$[Cl^-] = 2 \times [Ca^{2+}] + 2 \times [Mg^{2+}] + [Na^+] + [K^+] - [HCO_3^-] \quad (13)$$

and assuming charge balance:

$$\sum cations = \sum ions \quad (14)$$

However, errors associated with analytical procedures may introduce imbalances in the electrical charge. The charge-balance error (CBE) is one measure with its value in percent:

$$CBE = \frac{\sum cations - \left|\sum anions\right|}{\sum cations + \left|\sum anions\right|} \times 100 \quad (15)$$

CBE is a checksum to ensure CASPER is successfully representing all ions $\sum ions$ within the substrate that is being simulated. Determining the equilibrium solution composition allows prediction of calcite precipitation within the system through two key variables: temperature and ionic strength. The ionisation constant K_2, and calcite solubility product (K_c) are temperature dependent and are expressed as logarithmic values, pK, which are dependent on temperature and are introduced via the following equations.

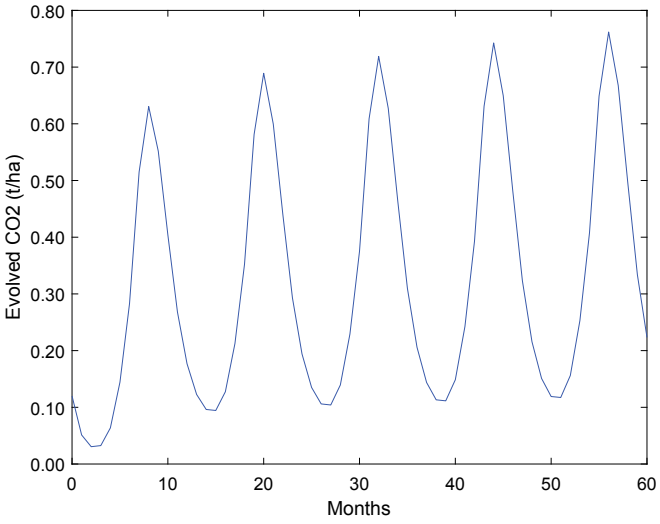

Fig. 2. CO_2 concentration in soil gas over 60 months.

$$pK_2 = \left(\frac{2902.39}{T}\right) + 0.02379\ T - 6.498 \quad (16)$$

Table 3
Model initial values.

Criteria	Value	Initial data setup
Soil Porosity	%	25 (Basaltic)
Moisture content	%	60 (Field capacity)
Clay content of the soil	%	0
DPM/RPM Ratio	< 0–1 >	1.44
Average monthly mean air temperature	ºC	ROTH C standard files
Soil Cover	Cover Material	ROTH C standard files
Monthly input of plant residue	t C ha^{-1}	0.065 (Managed grass)
Depth of soil layer sampled	cm	100
Organic compartments	t/ha	DPM 0; RPM 0; HUM 0; BIO 0; IOM 0
Silicate mineral stocks	t/ha	[Ca] 951.8; [Mg] 533.8; [Na] 284.7; [K] 120.7
Shell depth	mm	0.01
Substrate density	g/cm^3	2.7 (Basaltic)
Grain diameter	µm (mm)	100 (0.1)
Elemental weathering rate	mols m^{-2} s^{-1}	[Ca] 2.94 × 10^{-10}; [Mg] 6.47 × 10^{-10}; [Na] 0.203 × 10^{-10}; [K] 0.046 × 10^{-10}
Calculated monthly weathering rate	mol ha^{-1} mon^{-1}	[Ca] 472,470; [Mg] 1,039,755; [Na] 71,793; [K] 1123
Soil solution composition	mM	[Ca+] 0.97; [Mg+] 0.18; [Na+] 0.74; [K+] 55; [Cl−] 2.64; [HCO3-] 0.4; [CaCO3] 0
Soil pH	1–10	8
Atmospheric pressure	ATM	1

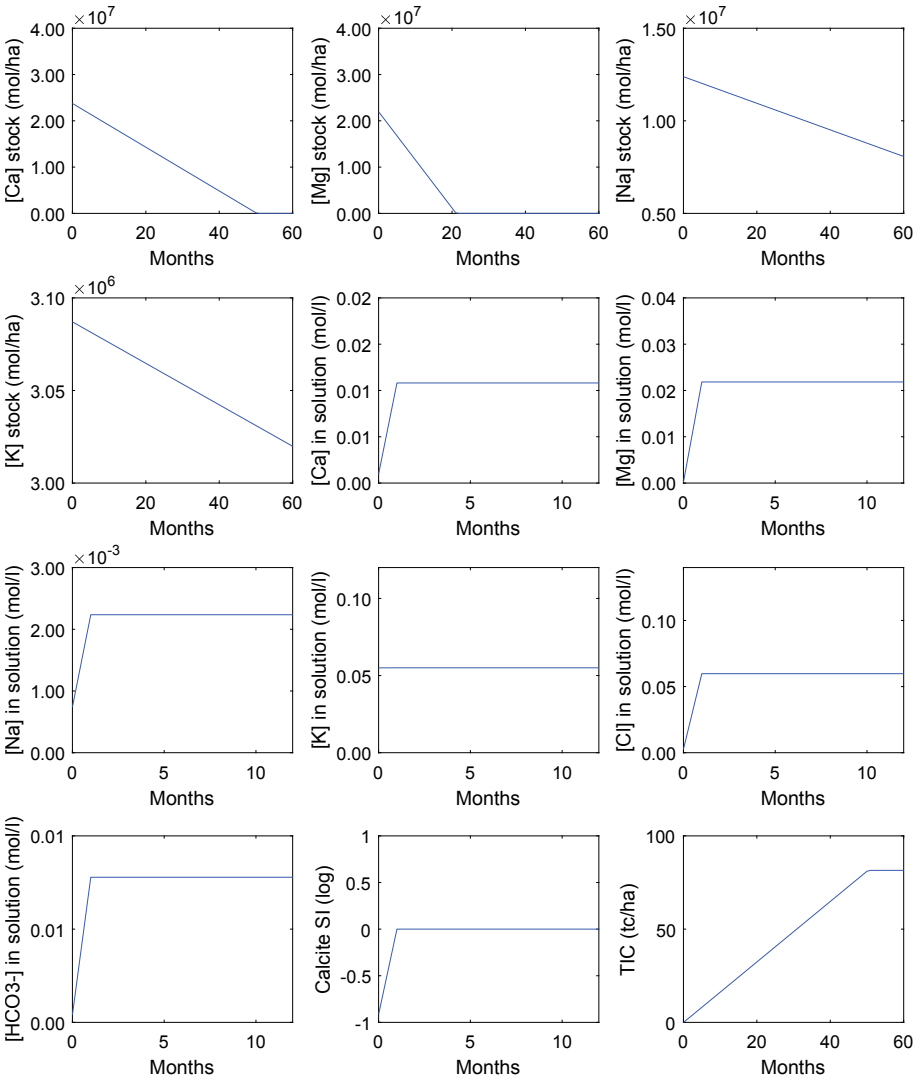

Fig. 3. Results of CASPER, illustrating state of elemental stocks, elements in solution and the calcite saturation index after 60 months (5 years).

where T is in the range of 273–323 K or 0–50 °C (Harned and Scholes, 1941). The dissociation constant of calcite is given by:

$$pK_c = 13.870 - (\frac{3059}{T}) + 0.04035\ T \tag{17}$$

Where T is in the range of 273–323 K or 0–50 °C (Jacobson and Langmuir, 1974). As the ionic strength increases, the activity of the species is reduced. Equations for equilibrium are correct when appropriately written in terms of activities:

$$fi\,[X] = (X) \tag{18}$$

where:

fi = Activity coefficient.
$[X]$ = molar concentration of X.
(X) = activity of ion X.

The Davies equation is used in order to determine the value of the activity coefficients (Panthi, 2003):

$$log\,(fi) = -0.5 \times Z_I^2(\frac{\sqrt{\mu}}{1+\sqrt{\mu}} - 0.3\mu) \times A \tag{19}$$

where $log\,(fi)$ is the logarithmic activity coefficient, Z_I^2 is the ion charge.

As the elements are released into solution, the ionic strength changes and is expressed in the model as:

$$I = \frac{1}{2}\sum_{i=1}^{n} c_i z_i^2 \tag{20}$$

where one half is because the quantities of total anions and cations are equal to maintain charge balance, the molar concentration of ion I in moles per litre or mol/l is defined as c_i, z_i is the ion charge number and all of the ions within the solution are summed appropriately. In more dilute solutions there is a lack of sensitivity towards ionic strength for activity coefficients, therefore the ionic strength can be approximated and still maintain appropriate and acceptable accuracy so that if only an approximate estimate of ionic strength is available, the activities can be determined. In natural water, the concentration of total inorganic dissolved solids can be used to estimate ionic strength (mol/l), S_d:

$$\mu = 2.5 \times 10^{-5} S_d \tag{21}$$

This relationship ceases once concentrations of 1000 mg/l are reached. Activities of 1 are assumed for water, solids and gases.

2.2.4. Calcite precipitation

Calcite precipitation is calculated using the (APHA, 2012) model,

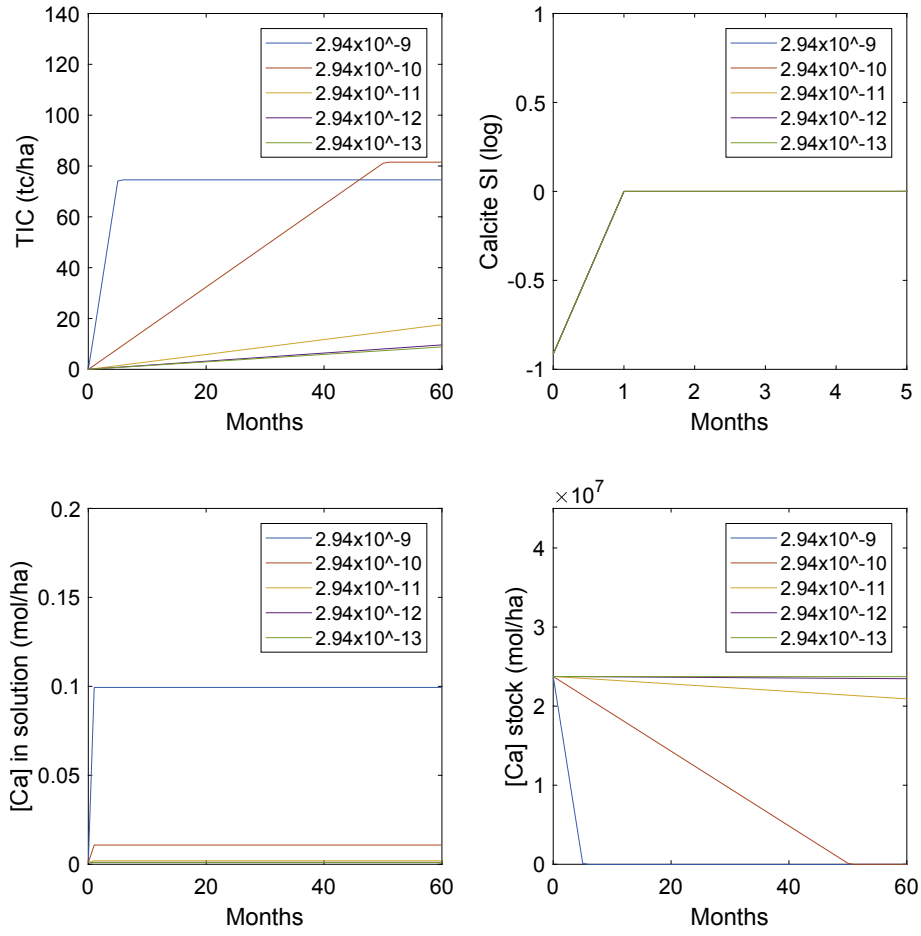

Fig. 4. Sensitivity results for scaled weathering rates after 60 months (5 years).

Table 4
Weathering rates of anorthite and diopside (Palandri and Kharaka, 2004).

Parameters	Anorthite (mol m^{-2} s^{-1})	Diopside (mol m^{-2} s^{-1})
Acidic soils	3.50×10^{-14}	6.36×10^{-14}
Neutral soils	9.12×10^{-14}	11.11×10^{-14}
Basic soils	11.15×10^{-14}	11.11×10^{-14}
Ca (%)	13.72	18.51
Mg (%)	0	11.22
Na (%)	0.41	0
K (%)	0	0

taking into account temperature and ionic strength to determine mineral saturation indices of the soil solution and so predicting the precipitation of calcite (Manning and Robinson, 1999). Mineral saturation indices (SI) are calculated as follows:

$$SI = \log(\frac{IAP}{K_{sp}}) \tag{22}$$

Ion activity product is abbreviated to IAP, K_{sp} refers to the mineral's solubility product (Drever, 1988). Instead of using the concentration as the measure of over or under-saturation, Langelier avoided the use of $CaCO_3$ concentration and instead used alkalinity and calcium concentration in order to determine the assumed pH level of water in terms of saturation of $CaCO_3$. This was known as the saturated pH value or pH_s:

$$pH_s = pK_2 - pK_c + \left[pCa_2{}^{+}\right] + \left[pHCO_3{}^{-}\right] + (5 \times log(fi)) \tag{23}$$

where $\left[pCa_2{}^{+}\right]$ and $\left[pHCO_3{}^{-}\right]$ are calcium and bicarbonate concentrations. Saturation states of minerals can be expressed as an appropriate saturation index. This is also known as the Langelier index and can be determined through the difference between actual values of water pH and pH_s that has been declared above:

$$SI = pH - pH_s \tag{24}$$

When the saturation index is zero, the mineral is saturated with respect to the solution. A mineral is supersaturated if the index has a positive number and is expected to precipitate, and undersaturated if it is a negative number and so is expected to dissolve.

2.3. Data collection for model start-up

In order for the model to accurately predict inorganic C as well as total C content, a number of specific criteria are required. Some RothC data have an impact on the variables in *CASPER* which can be acquired from a number of sources. For the purposes of this study, *CASPER* simulates a basaltic soil substrate, in which a soil is composed of dolerite mixed with organic matter to produce a layer 1 m thick. Dolerite (chemically and mineralogically identical to basalt) quarry fines were selected due to this particular aggregate possessing low embedded lifecycle emissions as it is a by-product of the construction industry. Average monthly mean air temperature directly affects the activity coefficients that determine theoretical pH (as illustrated in eqn. (23)) as well as the calcite SI within solution (eqn. (24)). Initial elemental compositions of the ions in solution that have been displaced from basaltic soil were taken from Benians et al. (1977). The variables that

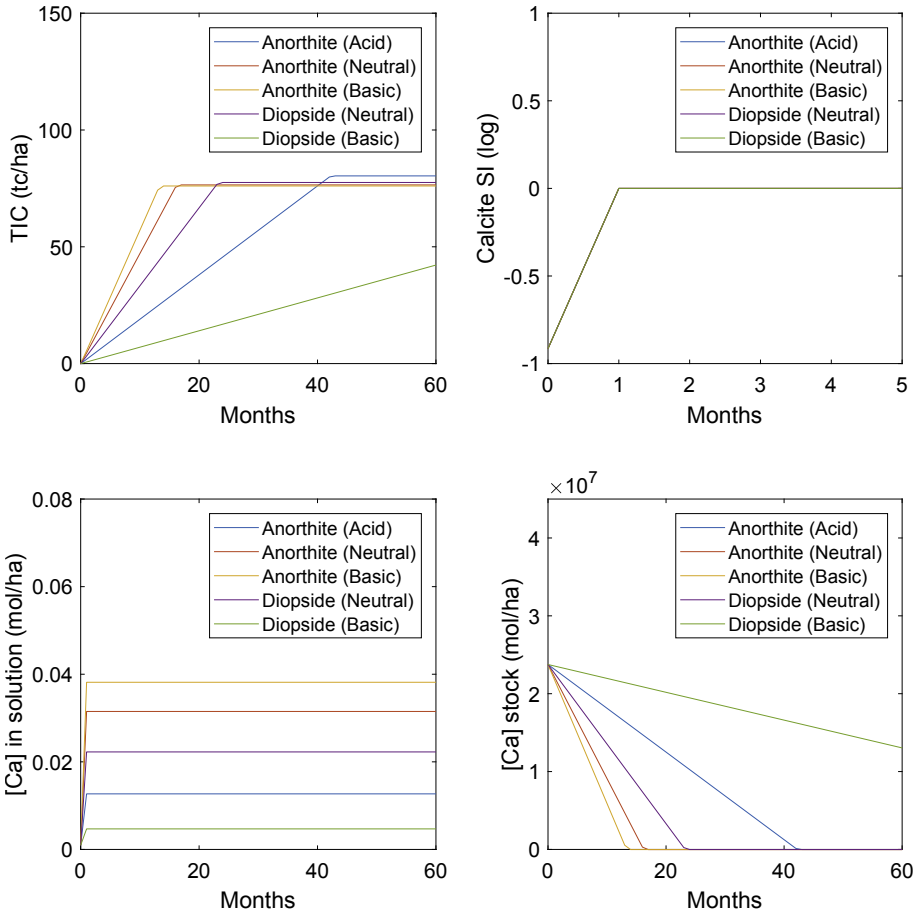

Fig. 5. Sensitivity results for comparison of similar mineral compositions against basic, neutral and acidic soil pH states.

are used are listed in Table 2. Appendix A-1 illustrates the theoretical relationship between grain diameter and particle shell depth to determine average weathering rates for basaltic soils per ha.

2.4. Initial model parameter values

Table 3 illustrates the model start-up values (initialisation). For monthly plant organic C input, *CASPER* uses continuous values for managed grass C inputs which were provided by Paustian et al. (2001), and which equal 0.78 t C ha yr^{-1} (0.065 t C ha $month^{-1}$). The user of the model should however use data that is available on the specific site of investigation. Farmyard manure RothC files have been used for the Rothamsted experiments to simulate compost decomposition.

Monthly time steps are used to illustrate seasonal variables. Soil solution composition is based on Benians et al. (1977) in mM. Average chemical compositions (wt%) of basalt were taken from Teir et al. (2005). The five organic C pools of RothC: DPM, RPM, HUM, BIO, and IOM are set to zero reflecting the construction of a newly engineered C capture soil profile, therefore the organic pools are not at equilibrium and there is no inert matter present. The weathering rates for individual minerals were taken from in situ experiments Hausrath et al. (2009). The weathering rates used in *CASPER* led to the following estimated release rates for a soil in which dolerite occurs to 1 m depth, in moles per hectare per month: Ca (472 470), Mg (1 039 755), Na (71 793) and K (1 123). Soil pH is set to 8 to reflect the relatively basic nature of the dolerite. *CASPER* assumes a single initial grain size. Grain diameter (G_d) is set to 0.1 mm (100 μm) with a 0.01 mm shell depth (*SD*). The DPM/RPM Ratio – an approximation of plant material decomposability that is entering and being influenced by the soil substrate, is set to the default of 59% DPM and 41% RPM, thus representing agricultural crops and improved grassland (C capture plots are simulated in the model with 10 cm of compost and rock dust mix). Air temperature is used where soil temperature data is not available. Temperature affects the rate of reaction in both organic and inorganic chemical processes and the standard RothC default files are used for temperature, soil cover and monthly input of plant residue.

3. Results

CASPER has been used initially to simulate an artificial soil of 1 ha of dolerite substrate which was mixed with an equal volume of green compost down to 1 m depth, over a period of 5 years (Manning et al., 2013). The results are shown in Figs. 2 and 3. There are a few important findings from this run. First, silicate stocks using the selected grain diameter (0.1 mm) and shell depth (0.01 mm) do not decrease significantly during the weathering process and in the short and medium term, the substrate will remain stable without significant soil pore cavities forming due to chemical weathering taking place.

3.1. Model state after initial run

Using the mineral dissolution rate given in Table 3, the solution attains calcite saturation during the first month, inducing calcite precipitation. Equilibrium within the system is achieved and the saturation index is equal to 0.

The ionic strength of the soil solution is sufficient to raise pH levels

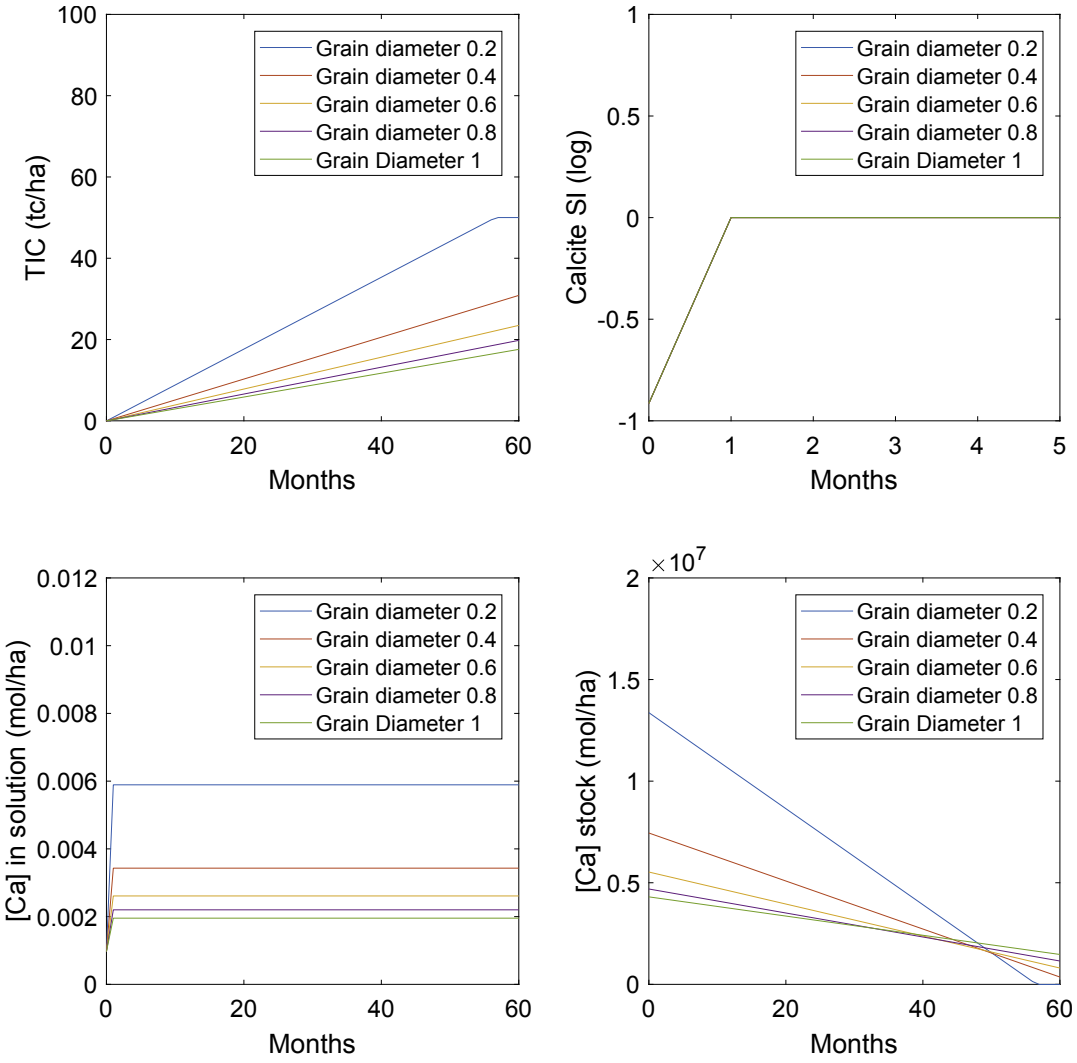

Fig. 6. Sensitivity results of variations in grain size (mm).

of the soil and to produce calcium carbonate as the calcite SI becomes positive during the 1st month. Maintaining SI at zero allows the amount of inorganic C precipitated as calcite to be determined. Fig. 3 illustrates the total amount of inorganic C that is precipitated over 5 years into the soil pores. Approximately 19.45 t CO_2 ha^{-1} were sequestered into the soil by precipitation of calcium carbonate over 5 years, corresponding to accumulation of approximately 81.51 tonnes of calcite ($CaCO_3$).

3.2. Sensitivity analysis

A sensitivity analysis was applied to selected variables to determine the lower and upper bounds in different soil states, and variations in input dissolution rates for anorthite (calcium end member of plagioclase feldspar: $CaAl_2Si_2O_8$) and diopside (a pyroxene: $CaMgSI_2O_6$), the two calcium silicate minerals that dominate in basalts and dolerites.

3.2.1. Variation in weathering rates

In order to test the calibration of the model, it was necessary to adjust the weathering rates within the bounds of current literature to determine variation in TIC accumulation. This was carried out through adjusting the higher power factor between 9 and 13. This range represents rates reported in the literature (in-situ and lab based). Fig. 4 illustrates the results of the weathering rate sensitivity analysis.

Weathering rates from basalt were compared with diopside and anorthite in basic, neutral and acidic states of soil pH (Palandri and Kharaka, 2004; Berg and Banwart, 2000). Due to the limited data available for bulk rock weathering rates, the weathering ratios of elements determined by Hausrath et al. (2009) in the initial results from basalt (controlled laboratory conditions) were maintained and normalised to calcium to ensure appropriate elemental behaviour of release was captured i.e. Ca(1), Mg(2.201), Na(0.069) and K(0.016) compared to the results of comparable silicate minerals in the analysis. Table 4 illustrates the parameters for simulating different soil characteristics, and Fig. 5 shows the model results. For diopside no data was available for basic pH conditions, so the value for neutral pH is assumed. During this particular run, it was noticeable that the increased weathering rates of the alternative substrates allowed higher concentration of elements to dissolve into solution. HCO_3^- was at its lowest by the time of saturation.

3.2.2. Variations in grain size

Further analysis on the effect of grain size was conducted. Grain size directly impacts the quantity of silicate stocks and the release rate of an element. The grain size was adjusted from the initial run (0.1) to

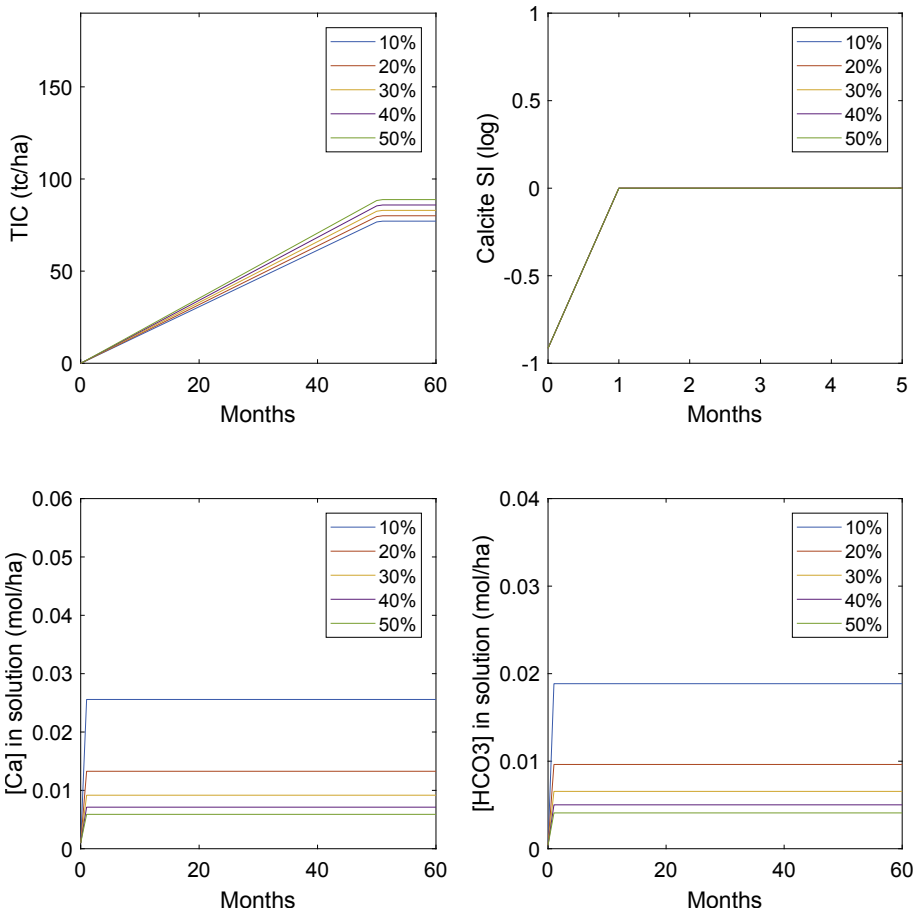

Fig. 7. Sensitivity results of soil porosity.

between 0.2 and 1 mm diameter. Shell depth was scaled in accordance with the increase in grain size to reflect larger soil particles. The results led to a steady decline of inorganic carbon content (TIC) as the grain size increases. This is most likely due to the reduced chemical weathering rate because of a reduced surface area available from number of grains per ha which also results in a reduced quantity of calcium in solution. The reserves of calcium silicates remain intact with a diameter of above 0.2 mm over 60 months, indicate that weathering and production of TIC is still ongoing during this period (see Fig. 6).

3.2.3. Moisture content and soil porosity

Adjustments in the moisture content and soil porosity were performed in order to determine sensitivity of key model variables based upon the simulation of random substrates (soil porosity) and atmospheric precipitation (moisture content). As expected, high soil porosity increases the production of calcite due to greater quantities of surface area being available although Calcite SI remains unchanged. When porosity is low, a higher quantity of calcium and bicarbonate in solution is observed (see Figs. 7 and 8).

In terms of moisture content, higher concentrations produce more calcite, and also the reduced head space causes an increase in partial pressure of CO_2 at moisture levels of 99%. Moisture content if reduced will cause an increase in the concentration of both HCO_3^- and Ca^{2+}.

3.3. Model comparisons

The results obtained from the model have been compared with observations from urban soils. Renforth et al. (2009) determined that 300 t C ha^{-1} to a depth of 3 m had entered the soil after 10 years, and reported an annual accumulation of 10 t C ha^{-1} (1 m soil depth) which corresponds to the modelled output from CASPER if the grain size is set to 0.2 mm with results of 50.0 t C ha^{-1}. At the urban Newcastle site previously studied, an annual rate of 23 t C ha^{-1} to 0.1 m depth was determined (Washbourne et al., 2012), which approximately equates to a 75 t C accumulation over 5 years. If the weathering rates of CASPER are adjusted to a power of 9, the results align well (74.55 t C ha^{-1}).

4. Discussion

4.1. Comparison of results to other models

There are currently no directly equivalent models to compare the results of *CASPER* and for the time being no possibility for comparison with independent existing experiments. Model accuracy depends mainly on weathering rates, representing the bulk dissolution rates of a mixture of minerals present within the soil. The model can predict average weathering rates inversely for basaltic (and other) substrates, by comparing the results of CASPER with appropriate field data. The focus of the original soil C models (all compatible with input to CASPER through their evolved CO_2 output) such as Roth C, CENTURY (Falloon and Smith, 2002) and DAISY (Mueller et al., 1996), was on fluctuations in SOC, representing decomposition of different C pools and evolutions of CO_2. While CASPER can predict mineral weathering and carbonate formation, validation from experimental observation is required to

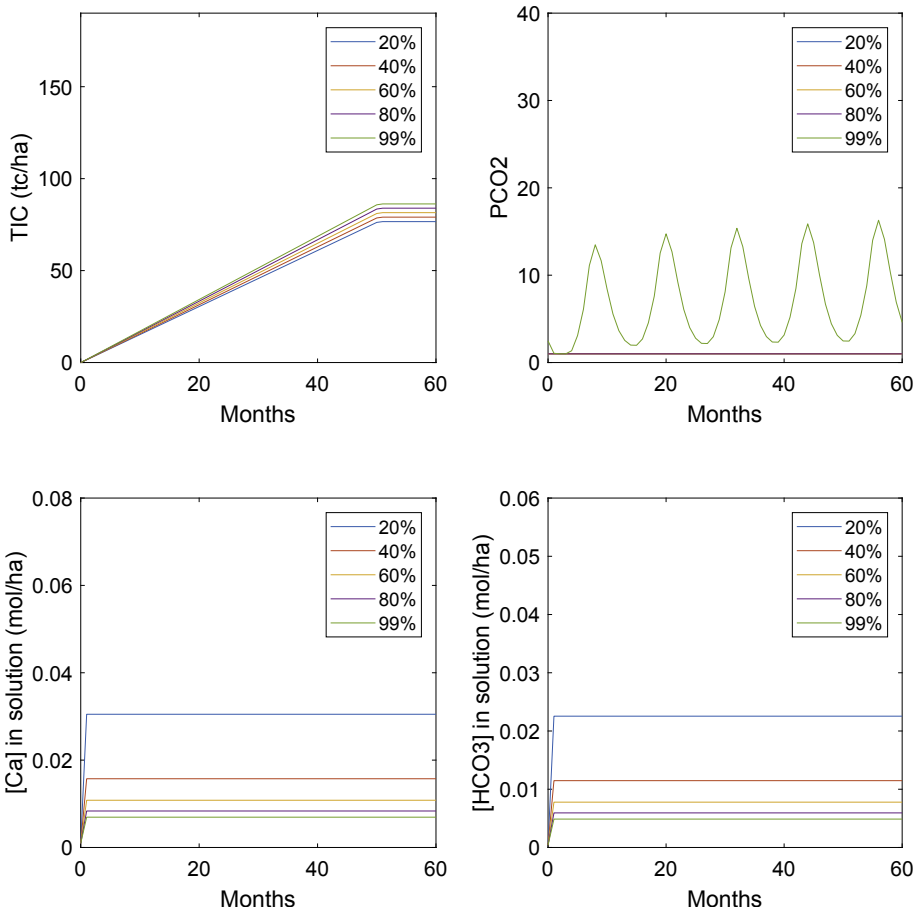

Fig. 8. Sensitivity results of moisture content.

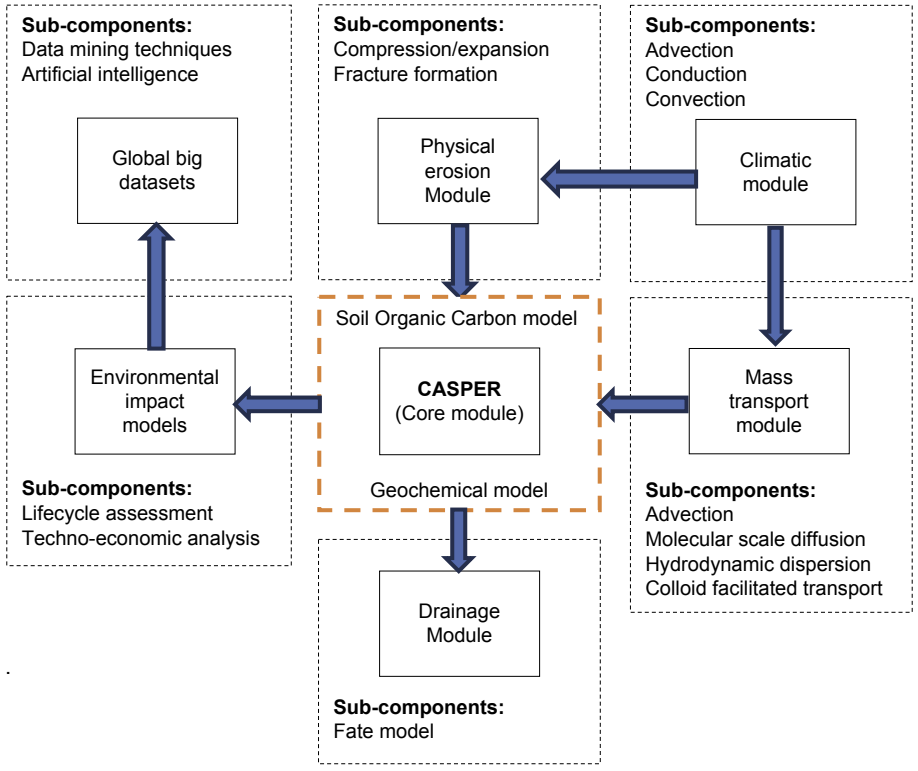

Fig. 9. Conceptual model of proposed CASPER modelling framework with full reactive transport modelling.

assess the model over a number of different sites with varying properties.

4.2. Adapting CASPER for reactive transport modelling and global studies

In *CASPER,* the dissolution of CO_2 and base cations is key to ensuring the model runs but the major driver is the determination of mineral weathering rates to derive the species in solution. CASPER is designed to be similar in scope to the existing models of soil organic C dynamics, which relate to land use. In principle, the accuracy of the weathering rate can improve through implementing reactive transport modelling techniques. These include incorporating additional geochemical reactions (in addition to the Arrhenius equation), mass transport of soil solution, the affect of temperature on the flow of water and medium deformation which can include the contraction and expansion of the substrate area. Weathering accuracy can be partially determined by reactive transport modelling to consider leaching and drainage. Although CASPER can be used to calculate the weathering rate when the rock is saturated in water as well as soil solution pH, it should then be possible to simulate drainage by determining the composition and density of the surrounding soil substrate and also to determine the flow rate of solution using data from existing models. A higher weathering rate will increase the rate of ionic strength provided that drainage rates of the soil solution are lower than dissolution rates. This will directly affect the production of calcite. Reactive transport modelling approaches can also be used to improve the accuracy of weathering rates based upon several key assumptions taking into account the physical deformation of artificial substrates. Currently, CASPER ignores physical weathering but indirectly replaces physical deformation (i.e. loss of substrate with calcite formation) as a form of simplification. In reality, it is necessary to treat both events separately, due to differences in density and textural variation of the parent material and carbonate. In addition, more extreme events such as abnormally high fluid pressure require special models that can determine physical deformation rates. It is important that these observations are considered when using CASPER, and other key effects including external environmental conditions including climate change should be estimated either separately from the model or be integrated into the existing system as an additional component. Fig. 9 illustrates a conceptual framework of a full reactive transport modelling approach. In addition, the output of CASPER is linked to key environmental and techno-economic assessment models, which can be used for input to global datasets that use big data techniques as well as a forecasting tool to determine carbon capture performance in the form of a plausible enhanced weathering approach.

4.3. Importance to enhanced weathering

One of the key barriers to ensuring enhanced weathering is a viable GGR reduction technology is the capability of estimating mineral dissolution kinetics, alongside lifecycle assessment approaches. Published rates of calcium dissolution cannot explain the rapid rates of carbonate C accumulation observed in field sites or artificial soils (Washbourne et al., 2015; Manning et al., 2013). A key use of our experimental data and modelling is, therefore, to infer effective rates for calcium dissolution, as it occurs in-situ in soil. The new dissolution rate for calcium under saturated conditions (using a weathering rate of 2.94×10^{-10} mol m^{-2} s^{-1}) is equal to 0.018 mol/l. This initial calibration enables further development and use of the model in increasingly complex and interesting GGR applications as well as supporting the latest target of zero net C emissions globally by 2050, as set out by IPCC (2018).

According to Renforth (2012), the UK has a high abundance of silicate mineral stocks sourced from igneous rock with a total area of 679,102 ha resulting in a combined carbon capture potential of 430 Gt of CO_2. The majority of these stocks are basic rocks (basaltic) with a carbonation potential of $\sim$0.3 t CO_2 t^{-1} mineral. Calcium is assumed to be available at around 10% of the total silicate mass. This type of rock is not just abundant in the UK but is also available globally due to basalt being one of the most common rock types in the Earth's crust (Beerling et al., 2018).

5. Conclusions

In the future, C sequestration through land management may be extended from a focus on organic decomposition to encompass the various effects of inorganic carbon precipitation, with the intention of creating an increased store of stable inorganic C. To guide this, new soil C models will be required. To this end we have extended the organic pools of the RothC soil model to create a new model: *CASPER*, which provides an explicit description of carbon accumulation as mineral calcite (calcium carbonate), using silicate weathering and a simulated calculated calcite saturation index (SI) to predict the precipitation of soil inorganic C (SIC) as $CaCO_3$. Simulations for the target substrate considered a model soil based on the calcium-silicate bearing rock dolerite. *CASPER* aims to provide a foundation in order to predict with a certain degree of accuracy values of inorganic carbon accumulation, following prediction of the point at which soil solution reaches calcite saturation. Taken together, *CASPER* offers a tool in which its predictions can provide an entry point for international and regional SIC assessments. It aims to quantify the contributions of enhanced weathering technologies and artificial soil products on a range of scales, given the occurrence of basaltic rocks over large areas of the continental crust. The model can also be used to simulate the behaviour of more typical soils, provided that knowledge of the soil mineralogical composition is known.

Acknowledgements

The authors wish to acknowledge UK funding of the SUCCESS project by the Engineering and Physical Sciences Research Council (EP/K034952/1).

Software availability

Software name CASPER (Carbonate Accumulation in Soils through the Prediction of Elemental Release)
Version v1.0.0.0
DeveloperBen Kolosz
E-mail address kolosz27@gmail.com
Year first available 2018
Required software Windows or Mac, Vensim PLE and Microsoft Excel/Office
Programming language Vensim
Availability and cost free of charge. Note that the piece of software (VENSIM) is a commercially available system dynamics model maker and does not feature source code (creating an independent program would be the next step) but all equations and variables are transparent and accessible through VENSIM PLE, allowing for complete replication and reuse in other programs or third party software where appropriate.
VENSIM PLE can be downloaded from the following website: http://vensim.com/free-download/. Model file and help has been uploaded to Mendeley Data.

Appendix A. Additional model detail

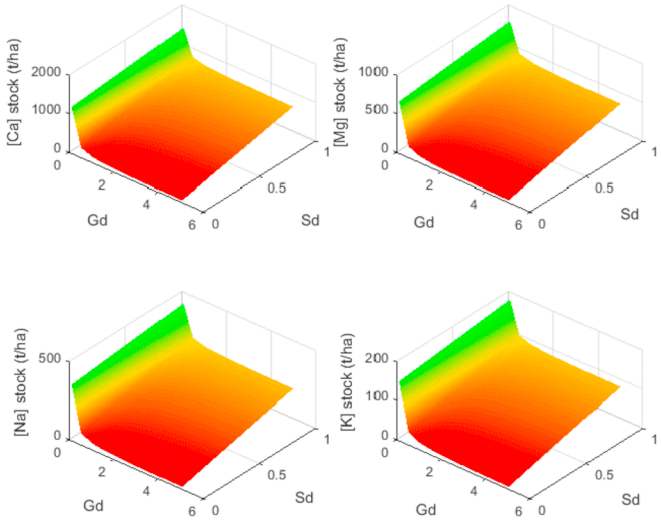

Fig. A 1. Relationship of grain diameter and particle shell depth to determine average elemental stocks of Ca, Mg, Na and K of basalt to 1m substrate

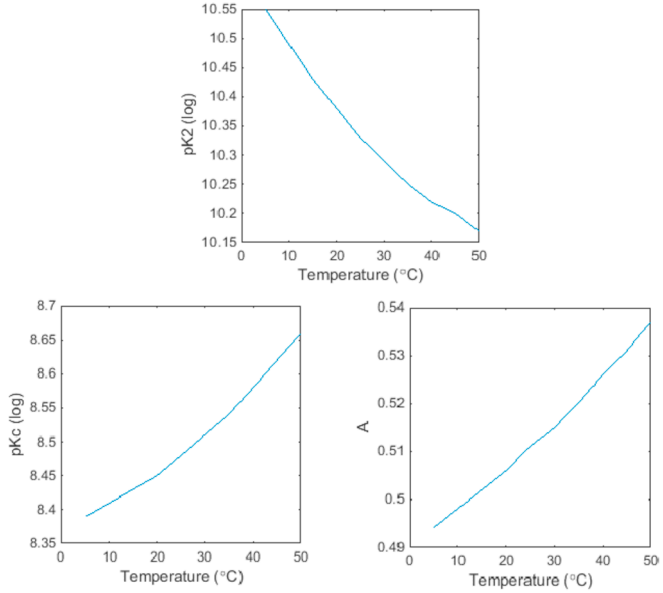

Fig. A 2. Relationship between the logarithmic values of the dissociation constants and temperature

References

APHA, 2012. Standard Methods for the Examination of Water and Wastewater. American Public Health Association, Washington DC, USA.

Beerling, D.J., Leake, J.R., Long, S.P., Scholes, J.D., Ton, J., Nelson, P.N., Bird, M., Kantzas, E., Taylor, L.L., Sarkar, B., 2018. Farming with crops and rocks to address global climate, food and soil security. Nat. plants 1.

Benians, G., Scullion, P., Fitzhugh, G., 1977. Concentrations and activities of ions in solutions displaced from basaltic soils. Eur. J. Soil Sci. 28, 454–461.

Berg, A., Banwart, S.A., 2000. Carbon dioxide mediated dissolution of Ca-feldspar: implications for silicate weathering. Chem. Geol. 163, 25–42.

Bonten, L.T., Reinds, G.J., Posch, M., 2016. A model to calculate effects of atmospheric deposition on soil acidification, eutrophication and carbon sequestration. Environ. Model. Software 79, 75–84.

Coleman, K., Jenkinson, D., 1996. RothC-26.3-A Model for the Turnover of Carbon in Soil. Evaluation of Soil Organic Matter Models. Springer.

Drever, J.I., 1988. The Geochemistry of Natural Waters. prentice Hall, Englewood Cliffs.

Eberlein, R.L., Peterson, D.W., 1992. Understanding models with Vensim™. Eur. J. Oper. Res. 59, 216–219.

Falloon, P., Smith, P., 2002. Simulating SOC changes in long-term experiments with RothC and CENTURY: model evaluation for a regional scale application. Soil Use Manag. 18, 101–111.

Harned, H.S., Scholes, S.R., 1941. The ionization constant of HCO3- from 0 to 50°. J. Am. Chem. Soc. 63, 1706–1709.

Hausrath, E., Neaman, A., Brantley, S., 2009. Elemental release rates from dissolving basalt and granite with and without organic ligands. Am. J. Sci. 309, 633–660.

IPCC, 2018. Global Warming of 1.5 °C. IPCC Special Report. Intergovernmental Panel on Climate Change, Geneva, Switzerland.

Jacobson, R.L., Langmuir, D., 1974. Dissociation constants of calcite and CaHC03+ from 0 to 50°C. Geochem. Cosmochim. Acta 38, 301–318.

Jorat, M., Kolosz, B., Sohi, S., LOPEZ-Capel, E., Manning, D.A., 2015a. Year. Changes in geotechnical properties of urban soils during carbonation. In: 15th Pan-American Conference on Soil Mechanics and Geotechnical Engineering, pp. 912–918.

Jorat, M.E., Goddard, M.A., Kolosz, B.W., Sohi, S., Manning, D.A.C., 2015b. Sustainable urban carbon capture: engineering soils for climate change (SUCCESS). In: 16th European Conference on Soil Mechanics and Geotechnical Engineering (XVI ECSMGE 2015). Edinburgh, United Kingdom.

Lal, R., Kimble, J., 2000. Inorganic Carbon and the Global C Cycle: Research and Development Priorities. Global Climate Change and Pedogenic Carbonates. CRC Press, Boca Raton, Fl, USA.

Lowenthal, R., Marais, G.V.R., 1976. Carbonate Chemistry of Aquatic Systems.

Manning, D., Robinson, N. Year, 1999. Leachate-mineral reactions: implications for drainage system stability and clogging. In: Proc. 7th Int. Landfill Symp. Cagliari, pp. 269–276.

Manning, D.A., Renforth, P., 2012. Passive sequestration of atmospheric CO2 through coupled plant-mineral reactions in urban soils. Environ. Sci. Technol. 47, 135–141.

Manning, D.A.C., Renforth, P., LOPEZ-Capel, E., Robertson, S., Ghazireh, N., 2013. Carbonate precipitation in artificial soils produced from basaltic quarry fines and composts: an opportunity for passive carbon sequestration. Int. J. Greenh. Gas Contr. 17, 309–317.

Marchant, B., Villanneau, E., Arrouays, D., Saby, N., Rawlins, B., 2015. Quantifying and mapping topsoil inorganic carbon concentrations and stocks: approaches tested in France. Soil Use Manag. 31, 29–38.

Mayes, W.M., Riley, A.L., Gomes, H.I., Brabham, P., Hamlyn, J., Pullin, H., Renforth, P., 2018. Atmospheric CO2 sequestration in iron and steel slag: consett, county durham, United Kingdom. Environ. Sci. Technol. 52, 7892–7900.

Mondini, C., Cayuela, M.L., Sinicco, T., Fornasier, F., Galvez, A., Sánchez-Monedero, M.A., 2017. Modification of the RothC model to simulate soil C mineralization of exogenous organic matter. Biogeosciences 14, 3253.

Morales-Flórez, V., Santos, A., Lemus, A., Esquivias, L., 2011. Artificial weathering pools of calcium-rich industrial waste for CO_2 sequestration. Chem. Eng. J. 166, 132–137.

Mueller, T., Jensen, L.S., Hansen, S., Nielsen, N., 1996. Simulating Soil Carbon and Nitrogen Dynamics with the Soil-plant-atmosphere System Model DAISY. Evaluation of Soil Organic Matter Models. Springer.

Palandri, J.L., Kharaka, Y.K., 2004. A Compilation of Rate Parameters of Water-mineral Interaction Kinetics for Application to Geochemical Modeling. GEOLOGICAL SURVEY MENLO PARK CA.

Panthi, S., 2003. Year. Carbonate chemistry and calcium carbonate saturation state of rural water supply projects in Nepal. In: Proceedings of the Seventh International Water Technology Conference, Cairo, Egypt, pp. 1–3.

Parton, W., 1996. The CENTURY Model. Evaluation of Soil Organic Matter Models. Springer.

Paustian, K., Parton, W.J., Persson, J., 1992. Modeling soil organic matter in organic-amended and nitrogen-fertilized long-term plots. Soil Sci. Soc. Am. J. 56, 476–488.

Paustian, L., Babcock, B., Hatfield, J.L., Lal, R., Mccarl, B.A., Mclaughlin, S., Mosier, A., Rice, C., Roberton, G., Rosenberg, N. Year, 2001. Agricultural mitigation of green-house gases: science and policy options. In: 2001 Conference Proceedings, First National Conference on Carbon Sequestration. Conference on Carbon Sequestration, Washington, DC.

Rawlins, B., Henrys, P., Breward, N., Robinson, D., Keith, A., Garcia-Bajo, M., 2011. The importance of inorganic carbon in soil carbon databases and stock estimates: a case study from England. Soil Use Manag. 27, 312–320.

Renforth, P., Edmondson, J., Leake, J.R., Gaston, K.J., Manning, D.A.C., 2011a. Designing a carbon capture function into urban soils. Proc. ICE - Urban Des. Plan. 164, 121–128.

Renforth, P., Manning, D.A.C., LOPEZ-Capel, E., 2009. Carbonate precipitation in artificial soils as a sink for atmospheric carbon dioxide. Appl. Geochem. 24, 1757–1764.

Renforth, P., Washbourne, C.L., Taylder, J., Manning, D.A.C., 2011b. Silicate production and availability for mineral carbonation. Environ. Sci. Technol. 45, 2035–2041.

Renforth, P., 2012. The potential of enhanced weathering in the UK. Int. J. Greenh. Gas Contr. 10, 229–243.

Sander, R., 2014. Compilation of Henry's law constants, version 3.99. Atmos. Chem. Phys. Discuss. 14, 29615–30521.

Skjemstad, J., Spouncer, L., Cowie, B., Swift, R., 2004. Calibration of the Rothamsted organic carbon turnover model (RothC ver. 26.3), using measurable soil organic carbon pools. Soil Res. 42, 79–88.

Smith, P., Smith, J.U., Powlson, D.S., Mcgill, W.B., Arah, J.R.M., Chertov, O.G., Coleman, K., Franko, U., Frolking, S., Jenkinson, D.S., Jensen, L.S., Kelly, R.H., KLEIN-Gunnewiek, H., Komarov, A.S., Li, C., Molina, J.A.E., Mueller, T., Parton, W.J., Thornley, J.H.M., Whitmore, A.P., 1997. A comparison of the performance of nine soil organic matter models using datasets from seven long-term experiments. Geoderma 81, 153–225.

Teir, S., Eloneva, S., Zevenhoven, R., 2005. Production of precipitated calcium carbonate from calcium silicates and carbon dioxide. Energy Convers. Manag. 46, 2954–2979.

Washbourne, C.-L., LOPEZ-Capel, E., Renforth, P., Ascough, P.L., Manning, D.A., 2015. Rapid removal of atmospheric CO2 by urban soils. Environ. Sci. Technol. 49, 5434–5440.

Washbourne, C.-L., Renforth, P., Manning, D., 2012. Investigating carbonate formation in urban soils as a method for capture and storage of atmospheric carbon. Sci. Total Environ. 431, 166–175.

Weber, W.J., Stumm, W., 1963. Mechanism of hydrogen ion buffering in natural waters. J. (Am. Water Works Assoc.) 55, 1553–1578.